UILU-ENG 84-3605

Report No. 105

# PREDICTING FATIGUE PROPERTIES THROUGH HARDNESS MEASUREMENTS

by

James C. McMahon and F. V. Lawrence
Department of Metallurgy and Mining Engineering, UIUC

A Report of the

MATERIALS ENGINEERING - MECHANICAL BEHAVIOR

College of Engineering, University of Illinois at Urbana-Champaign

February 1984

## ABSTRACT

The fatigue properties of steels can be estimated from their hardnesses just as tensile strength is commonly related to this familiar measurement. Knowledge of such material properties is required when making predictions of the fatigue resistance of weldments. The use of hardness measurements is not meant to replace actual fatigue testing. It is here proposed for the estimation of the fatigue properties of materials which are difficult and expensive to test, such as the HAZ (heat-affected zone) of welds. This paper examines and compares the commonly used relationships between hardness and fatigue properties and also investigates the applicability of these correlations to various steels over different ranges of strength.

TABLE OF CONTENTS

# LIST OF SYMBOLS

| | |
|---|---|
| $\underline{a}$ | Peterson's Material Constant |
| b | Fatigue strength exponent |
| c | Fatigue ductility exponent |
| E | Modulus of elasticity |
| H | Hardness |
| k | Stress relaxation exponent |
| $K_f$ | Fatigue notch factor |
| $k_{fmax}$ | Maximum fatigue notch factor |
| $L_l$, $L_u$ | Lower and upper life estimates |
| $N_I$, $N_p$, $N_T$ | Initiation, propagation, and total life |
| $N_f$ | Life to failure |
| $N_{tr}$ | Transition fatigue life |
| 2N | Reversals |
| r | Correlation coefficient |
| r | Notch root radius |
| $S_u$, $S_y$ | Ultimate and yield strength |
| $\Delta S$ | Remote stress range |
| t | Plate thickness |
| $\alpha$ | Geometry coefficient |
| $\epsilon_E$, $\epsilon_P$, $\epsilon_T$ | Elastic, plastic, and total strain |
| $\epsilon_f$ | True fracture ductility |
| $\epsilon'_f$ | Fatigue ductility coefficient |
| $\sigma_f$ | True fracture strength |
| $\sigma'_f$ | Fatigue strength coefficient |
| $\sigma_o$ | Mean Stress |

# LIST OF ABBREVIATIONS

| | |
|---|---|
| BM | Base Metal |
| CFS | Calculated fatigue strength |
| DPH | Diamond pyramid hardness (Vickers) |
| EFS | Estimated fatigue strength |
| Eq., Eqs. | Equation(s) |
| Fig., Figs. | Figure(s) |
| HAZ | Heat-Affected Zone |
| HB | Brinell hardness |
| log | Base-10 logarithm |
| mm | millimeters |
| MPa | $10^6$ Pascals |
| psi, ksi | Pounds and kips per square inch |
| RA | Reduction in area |
| SAE | Society of Automotive Engineers |
| TIG | Tungsten Inert Gas (welding) |
| WM | Weld metal |

# 1. INTRODUCTION

## 1.1 General

Weldments are often subjected to variable or repeated loadings and are consequently prone to fatigue failure. In the past, the fatigue resistance of welded joints has been studied through tests on full size weldments, a difficult and time consuming procedure. The fatigue properties of weld zones (such as the HAZ or weld metal) may be estimated from microhardness measurements made in the region of interest using relationships between hardness and fatigue properties, such as those developed by Landgraf [1] and Higashida [2].

## 1.2 Material Properties Required in the Estimation of Fatigue Resistance

The initiation-propagation model (or I-P model) developed by Lawrence et al. [3] predicts the total fatigue life ($N_T$) of weldments by combining estimates of the of the fatigue crack initiation life ($N_I$) and the fatigue crack propagation life ($N_p$). The I-P model is especially effective in the long-life regime where initiation life is more dominant (an important period which may be neglected by models based soley on crack propagation).

Fatigue cracks usually initiate at the most highly strained regions of a structure subjected to cyclic loading. Fig. 1 shows three possible sites of fatigue crack initiation in a butt weld. The fatigue cracks shown in Fig. 1 can be located in either the weld metal or the HAZ. The mechanical and fatigue properties of these regions are generally unavailable and difficult to obtain experimentally. To obtain the fatigue properties of the HAZ, one has to simulate the microstructure of the region in test specimens and perform the appropriate fatigue tests. These expensive and time consuming tasks can be avoided by estimating the required fatigue properties from hardness measurements.

The expression relating the total strain amplitude to the fatigue life is:

$$\frac{\Delta\epsilon_T}{2} = \frac{\sigma_f'}{E}(2N_f)^b + \epsilon_f'(2N_f)^c \quad (1)$$

where $E$ = Young's Modulus

$\sigma_f'$ = fatigue strength coefficient

$b$ = fatigue strength exponent

$\sigma_f'$ = fatigue ductility coefficient

$c$ = fatigue ductility exponent

The elastic and plastic strains are represented by the two terms on the right hand side of Eq. 1.

elastic strain $$\frac{\Delta\epsilon_E}{2} = \frac{\sigma_f'}{2}(2N_f)^b \quad (2)$$

plastic strain $$\frac{\Delta\epsilon_p}{2} = \epsilon_f'(2N_f)^c \quad (3)$$

The fatigue properties defined above are essential to the prediction of fatigue resistance. The I-P model uses a form of Basquin's law [4] to predict $N_I$.

$$\sigma_a = (\sigma_f' - \sigma_o)(2N_I)^b \quad (4)$$

where $\sigma_o$ is the mean stress. Rearranging Eq. 4 and using the fatigue notch factor ($K_f$) one obtains:

$$N_I = \left(\frac{\sigma_f' - \sigma_o}{\frac{\Delta S}{2} K_f}\right)^{-\frac{1}{b}} \quad (5)$$

where $\frac{\Delta S}{2}$ = remote stress range

The mean stress ($\sigma_o$) depends on residual stresses and the mean stress relaxation exponent ($k$). The value of the residual stress is limited by the yield strength of the base metal, which can be estimated from hardness. The fatigue

notch factor ($K_f$) and $K_{fmax}$ are related to strength and can also be derived from hardness measurements.

The properties required to estimate the fatigue resistance of weldments are summarized below:

1. The strain controlled fatigue properties: $\sigma'_f$, b, $\epsilon'_f$, and c.
2. The ultimate strength of the base metal and HAZ.
3. The yield strength of the base metal (used to estimate residual stresses).
4. The maximum fatigue notch factor, $K_{fmax}$.

## 1.3 Reported Correlations of Fatigue Properties with Tensile Properties and Hardness

### The Ultimate Strength as a Function of Hardness

Hardness is frequently used as a convenient and rapid indicator of tensile strength. The relationship between the Brinell Hardness (HB) and the ultimate strength of steel is well known [5, 6, 7, 8]:

$$S_u = 500\ HB \quad \text{(psi)} \qquad (6)$$

$$S_u = 3.45\ HM \quad \text{(MPa)}$$

The above relationship is important for this study because some of the relationships stem from the correlations between fatigue properties and the ultimate strength. The ultimate strength is plotted against hardness in Fig. 2 for the materials considered in this investigation.

### Fatigue Properties

Landgraf [1] studied the hardening process on the cyclic dependent deformation and fatigue behavior of steels and reported that fatigue properties could

be related to hardness, or in some cases, could be correlated to their monotonic counterparts such as: $\sigma_f'$ with $\sigma_f$; $\epsilon_f'$ with $\epsilon_f$; and n' with n. Relationships between fatigue properties and strength or hardness given by Socie [6] and Mitchell [7] include:

$$\sigma_f' = S_u + 50 \quad \text{(ksi)} \tag{7}$$

$$b = -1/6 \log (2\,\sigma_f/S_u) \tag{8}$$

$$\epsilon_f = \ln\left(\frac{1}{1 - RA}\right) \tag{9}$$

c: varies between -0.5 for hard steels and -0.7 for ductile steels (10)

$$\epsilon_{Total} = 1\% \text{ at 1000-2000 reversals for all steels} \tag{11}$$

The fatigue strength calculated at $10^6$ reversals has often been approximated as one-half the ultimate strength [6, 7]. A similar measure of endurance, called the fatigue limit, is reported by Cazuad [9] to be one-half the ultimate for wrought steels with ultimate strengths up to 1250 MPa (about 350 DPH). Cazuad also reported this ratio (fatigue limit to ultimate strength) to be as low as 0.25 for martensitic steels.

Higashida [2] examined the relationships of n', b, c, $2N_{tr}$, and k, with hardness for ASTM A36, and mild steel, and ASTM A514, a quenched and tempered steel. He combined his data for ASTM A36 and ASTM A514 with Landgraf's data [1] for hardened steels and concluded:

1. The cyclic strain hardening exponent (n') decreased with increasing hardness (see Fig. 3).
2. No trend occured for the fatigue strength exponent (b) or fatigue ductility exponent (c), however values were within the ranges defined by Eqs. 8 and 10 (see Figs. 4a and 4b).

3. The log of the transition fatigue life ($2N_{tr}$) decreased linearly with increasing hardness (see Fig. 5).
4. The mean stress relaxation exponent (k) depend more on strain amplitude and material than on hardness (see Fig. 6).

Lawrence et al. [10, 11] suggested the use of hardness to predict fatigue properties necessary for the prediction of the fatigue crack initiation life ($N_I$). They found the HAZ and weld metal fatigue properties are often similar to those of the base metal for mild steel weldments. They also used the ultimate strength to calculate the maximum value of the fatigue notch factor ($K_{fmax}$).

Chang [12], expanding upon the work of Lawrence [10], used Eqs. 5 through 8 to predict HAZ fatigue properties of weldments which were TIG or laser dressed (processes used to alter weld toe geometry). Chang also developed a relationship between the HAZ hardness and the base metal hardness (reported as H(HAZ) = 1.5 H(HAZ) and a relationship between the yield strength and the ultimate tensile strength.

In a recent study, Miller et al. [13] made a thorough examination of various relationships between monotonic and cyclic properties. Miller et al. found the correlations of $\sigma_f'$ and b with the ultimate strength to be statistically significant, but they questioned the practical utility of such relationships.

A summary of the reported relationships presented in this section is given on the following page:

Table 1. Important Relationships Reported by Previous Researchers.

| Relationship | Source(s) |
|---|---|
| $S_u$ - 500 HB (psi) | 5, 6, 7, 8 |
| $\sigma_f' = S_u + 50$ (ksi) | 6, 7 |
| $b = -\frac{1}{6}\log(\frac{2\sigma_f}{S_u})$ | 6, 7 |
| $\sigma_a = 0.5\ S_u$ at $10^6$ reversals | 6, 7 |
| H(HAZ) = 1.5H (BM) | 12 |

## 1.4 Intent of Study

The intent of this study was to investigate further the relationships between fatigue properties and hardness. It is hoped that such relationships will permit the rapid estimation of fatigue properties of weld zones, such as the grain coarsened HAZ, so to avoid the necessity of difficult and expensive direct mechanical determination. Relationships proposed by in the past were confirmed or refined. The fatigue strength coefficient ($\sigma_f'$) and the fatigue strength exponent (b) were of primary importance because of their usefulness in the prediction of the fatigue crack initiation life ($N_I$). A parameter called the calculated fatigue strength or CFS (based on both $\sigma_f'$ and b) was introduced to describe long life fatigue behavior as a function of hardness.

# 2. ESTIMATING FATIGUE PROPERTIES THROUGH HARDNESS MEASUREMENTS

## 2.1 Source of Data

The plain-plate steels considered in this study are listed in Table 2. The other sheet steels and high strength steels also listed in Table 2 were included in this study to see how well the developed fatigue property-hardness relationships extrapolated to higher hardness and thinner materials.

The steels were divided into the four categories: hot rolled, quenched and tempered, normalized, and cold drawn. These categories are identified in the figures of this study by separate symbols. The results available for simulated HAZ materials of these steels are identified by solid symbols.

Table 2. Steels, Hardness Ranges, and Data Sources.

| Steels | Hardness Range, DPH[1] | Source(s) |
|---|---|---|
| Quenched and Tempered Steels | | |
| ASTM A514 | 265-330 | 2, 20 |
| SAE 10B62 | 455 | 21 |
| SAE 1045 | 225-530 | 21 |
| SAE 1541F | 265-300 | 21 |
| SAE 4130 | 265-385 | 21 |
| SAE 4140 | 325 | 21 |
| SAE 4142 | 400-590 | 21 |
| SAE 4340 | 365-435 | 21, 25 |
| SAE 5160 | 455 | 21 |
| SAE 52100 | 550 | 21 |
| SAE 9262 | 285-435 | 21 |

1. Some hardnesses are converted to DPH from HB or $S_u$.

Table 2, Continued

| Steels | Hardness Range, DPH | Source(s) |
|---|---|---|
| Hot Rolled Steels | | |
| ASTM A36 | 140-170 | 2, 20, 26 |
| ASTM A516 | 165 | 22 |
| ASTM A588 | 210 | 20 |
| Manten[2] | 170 | 27 |
| RQC-100[3] | 265-300 | 21, 27 |
| R-100[4] | 240 | 21 |
| Gainex[5] | 148-154 | 21 |
| SAE 1005-1009 | 90 | 21 |
| SAE 1006 | 105 | 23 |
| SAE 1020 | 108 | 21 |
| SAE 30304 | 145-160 | 21 |
| SAE 4340 | 250 | 21 |
| SAE 950 | 150-250 | 14, 21, 23 |
| SAE 980 | 205-235 | 23 |
| Cold Drawn Steels | | |
| AM-350[6] | 525 | 21 |
| SAE 1005-1009 | 125 | 21 |
| SAE 30304 | 340 | 21 |
| SAE 1144 | 270 | 21 |
| Normalized Steels | | |
| SAE 1015 | 80 | 21 |
| Heat-Affected Zone (HAZ) | | |
| ASTM A36 | 233-255 | 2, 20 |
| ASTM A514 | 303-496 | 2, 20 |
| ASTM A516 | 215 | 22 |
| ASTM A588 | 252 | 20 |

2. Tradename - U.S. Steel Corporation.
3. Tradename - Bethlehem Steel Corporation.
4. Tradename - Republic Steel Corporation.
5. Tradename - Armco Steel Corporation.
6. Grade number - Allegheny Ludlum Steel Corporation.

## 2.2 Correlations of $\sigma_f'$ and b with Hardness

Both parameters of Basquin's equation (Eq. 4), the fatigue strength coefficient ($\sigma_f'$) and the fatigue strength exponent (b), are related to tensile strength and can be estimated from hardness measurements.

The variation of the fatigue strength coefficient ($\sigma_f'$) with hardness for the materials considered in this study is shown in Fig. 7 in which a linear relationship between $\sigma_f'$ and hardness can be observed. A regression analysis performed on the entire data yielded the following relationship:

$$\sigma_f' = 3.3\ \text{DPH} + 370 \cong 0.95\ S_u + 400 \quad \text{(MPa)} \tag{12}$$

$$r = 0.80 \text{ (correlation coefficient)}$$

Considering the hot rolled and quenched and tempered data separately provided the following relationships:

hot rolled:

$$\sigma_f' = 3.1\ \text{DPH} + 400 \cong 0.9\ S_u + 400 \quad \text{(MPa)} \tag{13}$$

$$r = 0.82$$

quenched and tempered:

$$\sigma_f' = 3.1\ \text{DPH} + 500 \cong 0.9\ S_u + 500 \quad \text{(MPa)} \tag{14}$$

$$r = 0.87$$

The cold drawn data deviate considerably from the central tendency of $\sigma_f'$ shown Fig. 7 and were not used in the above regression analyses. Reported values of the fatigue strength coefficients of thin sheet were very high and were also excluded [13, 14]. The fatigue properties of thin sheet will be discussed in Sec. 3.4.

The relationship presented for all steels (Eq. 12) is similar to the often used expression for estimating the fatigue strength coefficient suggested by Landgraf [1]:

$$\sigma_f' \cong \sigma_f \text{ (true fracture strength)}$$

$$\sigma_f' \cong S_u + 50 = DPH/2 + 50 \qquad \text{(ksi)}$$

$$\sigma_f' \cong S_u + 345 = 3.45\ DPH + 345 \qquad \text{(MPa)} \qquad (7)$$

The regression lines (Eqs. 13 and 14) are shown together with the above approximation (Eqs. 7) in Fig. 7.

The fatigue strength exponent (b) is plotted against hardness in Fig. 8. The scatter for b is greater than that observed for $\sigma_f'$ (compare Figs. 7 and 8). There is a general trend of b decreasing in absolute value with increasing hardness. More scatter is apparent at low hardnesses than at higher hardnesses where b tends to become constant at a value of about -0.08 $\pm$0.01.

A relationship commonly used to relate b to the ultimate strength (or hardness) is:

$$b = -1/6 \log \left(\frac{2\sigma_f'}{S_u}\right) = -1/6 \log \left(\frac{2\ DPH + 1380}{DPH}\right)$$

The origin of the above equation is as follows: The exponent b is the slope of the elastic portion of the strain life curve in log-log coordinates (Eq. 2). If two points of this line can be defined, then one can determine the slope b. Two points on the elastic strain line are: the fatigue strength coefficient (at 1 reversal) and the fatigue strength at $10^6$ reversals. The coefficient $\sigma_f'$ and $\sigma_a$ at $10^6$ reversals can both be expressed in terms of strength (see Table 1).

$$\sigma_f' = S_u + 345 \qquad \text{(MPa)} \qquad (7)$$

$$\text{and } \sigma_a \text{ at } 10^6 \text{ rev.} = 0.5\ S_u \qquad (15)$$

The slope between these two points is b. Solving for b:

$$b = -1/6 \log \left(\frac{\sigma_f'}{\sigma_a \text{ at } 10^6 \text{ reversals}}\right) \qquad (16)$$

When Eqs. 7 and 15 are substituted into Eq. 16 one obtains:

$$b = -1/6 \log \left(\frac{S_u + 50}{S_u/2}\right) \quad (S_u \text{ in ksi}) \tag{17}$$

which is the often used relationship for b. This equation for b is shown as Eq. 1 in Fig. 8. Alternative forms of this relationship will be discussed in Sec. 2.3.

## 2.3 Correlation of the Fatigue Strength Calculated at $10^6$ Reversals with Hardness

In the previous section, correlations between $\sigma_f'$ and b and hardness were considered. The fatigue properties, $\sigma_f'$ and b, result from a linear regression analysis of strain life data. The slope and intercept of the best fit line of the elastic strain life data are b and $\sigma_f'$. With the addition of each data point, the calculated values of both $\sigma_f'$ and b change slightly; and these changes are coupled. For example, if $\sigma_f'$ increase then b will generally decrease (become more negative) as shown schematically in Fig. 9. These related changes observed in $\sigma_f'$ and b suggest the following: $\sigma_f'$ and b taken as a pair could be better used to describe the long life fatigue strength as a function of hardness. To test this idea, the fatigue strength at a standard life of $10^6$ reversals (termed the calculated fatigue strength or CFS) was plotted against hardness in Fig. 10. By defining the calculated fatigue strength is:

$$CFS = \sigma_f' (10^6)^b \tag{18}$$

The best-fit relationship between the CFS and hardness is:

$$CFS = 1.50 \text{ DPH} \quad \text{(MPa)} \tag{19}$$

or

$$CFS = 1.22 \text{ DPH} \quad \text{(ksi)}$$

$$r = 0.90$$

Fig. 10 also displays the line representing the relationship of Eq. 15:

$$\sigma_a \text{ at } 10^6 \text{ reversals} = 0.5\ S_u \qquad (15)$$

This reported relationship (Eq. 15) overestimates the calculated fatigue strength by 15% for nearly all the steels considered in this study (see Fig. 10). The difference between Eqs. 15 and 19 suggests that the relationship of the fatigue strength exponent (b) with hardness, which is dependent upon the estimate of the fatigue strength at $10^6$ reversals, can be improved as a consequence.

Alternative Relationship for the Fatigue Strength Exponent

An equation for the fatigue strength exponent can be developed using the relationship between the calculated fatigue strength and hardness. The equation for b noted before was Eq. 8, which follows the trend of the observed data, but tends to underestimate b (in absolute value). This equation was based on the emperical rules established for $\sigma_f'$ and the calculated fatigue strength at $10^6$ reversals. The relationships established for $\sigma_f'$ and CFS in this study (Eqs. 12-14 and 19) suggest a different relationship for the fatigue strength exponent (b):

$$b = -1/6 \log (A + B/DPH) \qquad (20)$$

Best-fit solutions for the parameters A and B in the above equation are given in Table 3.

Table 3. Parameters for Eq. 20.

| Data Group | A | B |
|---|---|---|
| equation 8 or 17 | 2 | 200 |
| all data considered | 2.1 | 266 |
| quenched and temp. steels | 2.4 | 308 |
| hot rolled steels | 2 | 200 |

The greatest scatter in the data shown in Fig. 8 is observed at low hardnesses. At higher hardnesses the quenched and tempered solution (A = 2.4, B = 308) agrees with the findings of Higashida [2]. It is the behavior of Eq. 20 to become constant at high hardnesses (> 300 DPH), as does the observed data, regardless of which set of parameters are used.

## 2.4 Correlations of Other Fatigue Properties with Hardness

### The Transition Fatigue Life

The transition fatigue life, $2N_{tr}$, is the life (reversals) at which the plastic and elastic strains are equal. From Eqs. 2 and 3:

elastic strain: $$\frac{\Delta\epsilon_E}{2} = \frac{\sigma'_f}{E}(2N_f)^b \tag{2}$$

plastic strain: $$\frac{\Delta\epsilon_E}{2} = \epsilon'_f (2N_f)^c \tag{3}$$

where $\epsilon'_f$ = the fatigue ductility coefficient

$c$ = the fatigue ductility exponent

By equating these two strains and solving for $2N_{tr}$, one obtains:

$$2N_{tr} = \left(\frac{E\epsilon'_f}{\sigma'_f}\right)^{\frac{1}{b-c}} \tag{21}$$

The transition fatigue life ($2N_{tr}$) may be used to compare strength and ductile behavior in fatigue resistance. Elastic strain is predominant at lives greater than $2N_{tr}$; whereas, plastic strain has greater influence at lives less than $2N_{tr}$. The knowledge of the transition fatigue life allows one to estimate the relative importance of the initiation (elastic behavior) and propagation (plastic behavior) stages of fatigue crack growth.

The transition fatigue life is plotted against hardness on semi-log coordinates in Fig. 11. There is a linear trend confirming the observations made by Landgraf [1] and Higishida [2] that the log of the transition fatigue life

decreases linearly with hardness. There is a slight difference between the quenched and tempered steels and the hot rolled steels. The results can be divided into two different groups, represented by the equations:

quenched and tempered: $$2N_{tr} = 6.2 \times 10^5 \exp(-0.016\ DPH) \quad (22)$$

hot rolled: $$2N_{tr} = 5.4 \times 10^5 \exp(-0.019\ DPH) \quad (23)$$

Ignoring the above difference, one can consider all steels to follow the same trend. The transition fatigue life, $2N_{tr}$, expressed as a single function of hardness, is:

all steels: $$2N_{tr} = 5.7 \times 10^5 \exp(-0.017\ DPH) \quad (24)$$

The Fatigue Notch Factor

Hardness (or ultimate strength) may be used to predict the fatigue notch factor, $K_f$. The fatigue notch factor varies between 1.0 and $K_t$ (the theoretical stress concentration factor). One estimate of $K_f$ is [15]:

$$K_f = 1 + \frac{K_t - 1}{1 + \underline{a}/r} \quad (25)$$

where r is the notch radius and $\underline{a}$ is Peterson's constant [15]. For heat treated steels:

$$\underline{a} = 10^{-3} \left(\frac{300}{S_u}\right)^{1.8} \quad (\underline{a} \text{ in inches, } S_u \text{ in ksi}) \quad (26)$$

or

$$\underline{a} = 0.025 \left(\frac{2070}{S_u}\right)^{1.8} \quad (\underline{a} \text{ in mm, } S_u \text{ in MPa})$$

For weldments, all possible radii are considered present. Therefore, $K_f$ has a maximum value which can be used for design. This maximum value, $K_{f\text{-max}}$, occurs when $\underline{a} = r$ [16].

$$K_{f\text{-max}} = 1 + 0.093\ \alpha\ (S_u)^{0.9}\ t^{0.5} \quad (27)$$

where $\alpha$ is a constant dependent on the specimen geometry, t is the plate thickness (in inches), and $S_u$ is measured in ksi. By combining Eqs. 6 and 27 one obtains:

$$K_{f\text{-}max} = 1 + 0.0498\ \alpha(DPH)^{0.9}\ t^{0.5} \tag{28}$$

Thus Eq. 28 defines $K_{f\text{-}max}$ as a function of hardness for a given plate thickness and geometry.

# 3. DISCUSSION

## 3.1 Comparison of Present and Previous Relationships

Table 4 compares the relationships reported in the past to those established by this study. The relationships for $S_u$ and $\sigma_f'$, in terms of hardness, determined in the present study were in agreement with relationships reported by previous researchers. This study showed that the fatigue strength calculated at $10^6$ reversals was approximately 0.435 $S_u$ rather than 0.5 $S_u$ as had been reported in the past for wrought steels (see Fig. 10). An alternative relationship between the fatigue strength exponent (b) and hardness was developed in this study using the fact that the conventional estimate of b (Eq. 8) assumed that the CFS equaled one-half the ultimate strength; whereas, this study found the above mentioned 0.435 $S_u$ to be more accurate.

Table 4. Comparison of Previous and Present Relationships

| Property | Previous Relationship | Present Study |
|---|---|---|
| $S_u$ (ksi) | $S_u = 0.5$ DPH [5, 6, 7, 8]<br>$S_u = 0.5$ HB | $S_u = 0.5$ DPH |
| $S_u$ (MPa) | $S_u = 3.45$ DPH | $S_u = 3.45$ DPH |
| $\sigma_f'$ (MPa) | $\sigma_f' = S_u + 345$ [6, 7] | $\sigma_f' = 0.95\ S_u + 370$<br>$= 3.3$ DPH $+ 370$ |
| b ($S_u$ in MPa) | $b = -\frac{1}{6}\log(2.0 + \frac{690}{S_u})$ [6, 7]<br>$= -\frac{1}{6}\log(2.0 + \frac{200}{\text{DPH}})$ | $b = -\frac{1}{6}\log(2.1 + \frac{917}{S_u})$<br>$= -\frac{1}{6}\log(2.1 + \frac{266}{\text{DPH}})$ |
| $\sigma_a$ (at $10^6$ reversals) (MPa) | $\sigma_a = 0.50\ S_u$ [6, 7]<br>$= 1.72$ DPH | $\sigma_a = 0.435\ S_u$<br>$= 1.50$ DPH |

## 3.2 Predicting the Hardness of the Heat-Affected Zone

Simulated HAZ fatigue data were included in this study to determine if the relationships between hardness and fatigue properties established for base metals are also applicable to their heat-affected zones. The HAZ is important to the study of the fatigue of weldments as is shown by the possible crack paths sketched in Fig. 1.

Bibby [17] proposed that the hardness of the heat-affected zone could be predicted using the "weld test method" developed by Stout [18], in which the material chemistry, plate thickness, geometry, and heat input were found to be important parameters in predicting the HAZ hardness. Chang [12] suggested a simpler correlation which relates the strength of the HAZ to that of the base metal (BM). Chang considered only fusion welds of steel plate and found:

$$S_u \text{ (HAZ)} = 1.5\ S_u \text{ (BM)} \tag{29}$$

Eq. 29 implies that the hardness of the HAZ should be related to the hardness of the base metal:

$$H \text{ (HAZ)} = 1.5\ H \text{ (BM)} \tag{30}$$

This relationship was tested by polishing sections of weldments from several structural steels, such as ASTM A-36 and ASTM A-514. The hardness measured in the heat-affected zones and base metals are plotted in Fig. 12. A range of hardnesses and an average value are shown for some data points because these weldments had two or more heat-affected zones with differing hardnesses.

The relationship between the base metal and HAZ hardness reported by Chang (Eq. 30) is confirmed in Fig. 12, but more scatter is observed than originally observed by Chang. The multitude of welding parameters (material, thickness, geometry, heat input, etc.) prohibits the exact correlation suggested by Eqs. 29 and 30. Further study will be required to develop a single parameter that could be used to predict the HAZ hardness. The cooling rate

parameter should be considered as Bibby suggested, because the resultant microstructure and hardness of the HAZ is governed by the cooling rate the HA7 experiences during after welding.

## 3.3 Estimating Yield Strength from Tensile Strength

Fatigue life prediction methods usually require knowledge of the state of residual stress in the weld. When the heat-affected zone residual stresses of weldments are unknown, they are often assumed to be equal to the yield strength of the surrounding base metal [16]. This assumption is roughly correct for residual stresses of as-welded or over-stressed weldments [16]. It is possible to estimate the yield strength of a steel from its ultimate strength, and if this correlation is known, then one can use the relationship to find the dependence of yield strength on hardness.

Chang [12] studied the relation between yield strength and ultimate strength for three different types of steel: hot rolled, normalized (870 C°), and quenched and tempered (430 C°). The linear relationships he found are listed together with yield strength data for hot-rolled carbon steel bars [5] in Table 5 below.

Table 5. Yield Strength Dependence on Ultimate Strength for Steels in Different Conditions.

| Steel Group/ref. | $S_u$ Range (MPa) | $S_y$ as a function of $S_u$ (MPa) | $S_y$ as a function of hardness (DPH) |
|---|---|---|---|
| Hot Rolled/[12, 19] | 296-552 | $S_y = 5/9\ S_u$ | $= 1.92$ DPH |
| Normalized/[12, 19] | 633-1276 | $S_y = 7/9\ S_u - 138$ | $= 2.68$ DPH $- 138$ |
| Quenched & Temp./[12, 19] | 758-1469 | $S_y = 1.2\ S_u - 345$ | $= 4.14$ DPH $- 345$ |
| Hot Rolled Bars/[5] | 350-950 | $S_y = 5/8\ S_u$ | $= 2.16$ DPH |

Chang's original data are plotted in Fig. 13 along with other yield strength data of steels considered in this study. The relationships listed in Table 5 were derived by Chang using isolated studies which considered a limited number of materials. Only data for the quenched and tempered group closely followed the relationship proposed by Chang, but the general trends reported by Chang seem to be followed by the other groups of steels considered (see Fig. 13).

## 3.4 Utility of the Calculated Fatigue Strength Approach

In a comprehensive study of the fatigue of sheet and plate steels, Miller [13] questioned the usefulness of correlating the fatigue strength coefficient ($\sigma_f'$) and the fatigue strength exponent (b) with monotonic properties. Similarly, Smith [14] observed a wide variability in values of $\sigma_f'$ and b occurs for thin sheet steel. The usefulness of the calculated fatigue strength (CFS) is illustrated by Miller's data shown in Fig. 14 where both $\sigma_f'$ and CFS are plotted against approximate hardness (only strength data were available from this reference). As Miller reported, no trend occured for $\sigma_f'$; in fact, all values of the fatigue strength coefficient ($\sigma_f'$) were higher than predicted by Eq. 7. However, the calculated fatigue strength (CFS) follows the trend shown by other materials. Obviously, each metal of this data group which had a higher than predicted $\sigma_f'$ also had a high value of b. This compensation resulted in a calculated fatigue strength (CFS) which was more clearly a function of hardness; thus, confirming the idea of Sec. 2.4 that $\sigma_f'$ and b are more useful when taken as a pair (in describing long-life fatigue behavior) and that variations of $\sigma_f'$ and b often are coupled.

This phenomenon was also observed for cold drawn data (marked as triangles in Figs. 7 and 10). Note the scatter these data display when the fatigue strength coefficient is correlated with hardness in Fig. 7; whereas, the calcu-

lated fatigue strengths of the cold drawn materials are within the range observed for the other steels (see Fig. 10).

This study presented relationships for $\sigma_f'$ and b as functions of hardness which can be used to estimate the fatigue strength at $10^6$ reversals. This estimate, which will be termed the EFS, was made for each steel considered in this study from $\sigma_f'$ and b values estimated from hardness (as opposed to measured values). The EFS is plotted against the CFS, which is calculated from reported measurements of $\sigma_f'$ and b, in Fig. 15. The deviation of the EFS from the CFS represents the possible error when making calculations of the fatigue strength at $10^6$ reversals based on values of $\sigma_f'$ and b estimated from hardness measurements.

Fig. 15 shows that one should expect at least a $\pm$15% uncertainty in the fatigue strength estimated solely on the basis of hardness. For an example, consider a hot rolled steel with a hardness of 200 DPH. The values of $\sigma_f'$, b, and EFS of this steel may be estimated from hardness using Eqs. 17 and 20:

$$\sigma_f' = 1030 \text{ MPa} \quad b = -0.089$$

$$\text{EFS} = \sigma_f' (10^6)^b = 301 \text{ MPa}$$

It is possible that the actual properties of this steel could be:

$$\sigma_f' = 1000 \text{ MPa} \quad b = -0.095$$

from Eq. 18: $$\text{CFS} = \sigma_f' (10^6)^b = 269 \text{ MPa}$$

resulting in an error of 12% in the fatigue strength at $10^6$ reversals. The fatigue life at a stress level of 301 MPa would be about 280,000 reversals which is lower than the expected value of the one million reversals by a factor of 3.6. A similar uncertainty of life would be expected if one underestimated the CFS, rather than overestimated as described above. The data which lie outside the $\pm$15% bands can be attributed to the variability in b observed at low hardnesses.

# 4. SUMMARY AND CONCLUSIONS

## 4.1 Summary

Hardness can be used to estimate fatigue properties, especially the fatigue strength coefficient ($\sigma_f'$), the calculated fatigue strength (CFS), and the transition fatigue life ($2N_{tr}$). Some of the relationships extrapolate well to steels of higher hardness, especially the relationships correlating $S_u$, $\sigma_f'$, and CFS with hardness. The fatigue properties of thin sheet and cold drawn steels did not follow the trends observed for plain plate steels. In these cases, the CFS approach, as described in Sec. 3.4, facilitated the notion of predicting the fatigue properties from hardness, however an error of 15% in fatigue strength or a factor of four in life must be expected when using this approach.

Not enough data was available to make separate analyses for the HAZ materials, but it was observed that the HAZ data followed the same trends shown by the base metal data. Thus, using hardness measurements to estimate fatigue properties of HAZ materials is more accurate than assuming their properties to be the same as the base metal properties. Naturally, making hardness measurements is far easier and quicker than the fatigue testing of simulated HAZ materials.

## 4.2 Conclusions

1. Hardness (HB or DPH) can be used to approximate the ultimate tensile strength (up to 500 DPH) and the fatigue strength coefficient ($\sigma_f'$) of wrought steels. The fatigue strength exponent (b) does not correlate well with hardness, but $\sigma_f'$ and b can be taken as a pair to form the CFS which does correlate with hardness. The CFS reduces the scatter observed for cold drawn steel and thin sheet steel data.

2. An error of ±15% in the fatigue strength at $10^6$ reversals estimated from hardness can produce a factor of 4 error in life calculations. These errors may be considered high, but are reasonable for initial estimates of the fatigue resistance which is based soley on hardness measurements.

3. The fatigue properties of the heat-affected zones can be calculated from the same relationships established for base metals. Furthermore, the hardness of the HAZ can be predicted from the base metal hardness, but perhaps not with the accuracy suggested by Chang [12].

4. The yield strength of steels was much more variable than Chang suggested; only the yield strengths of quenched and tempered steels correlated closely with hardness.

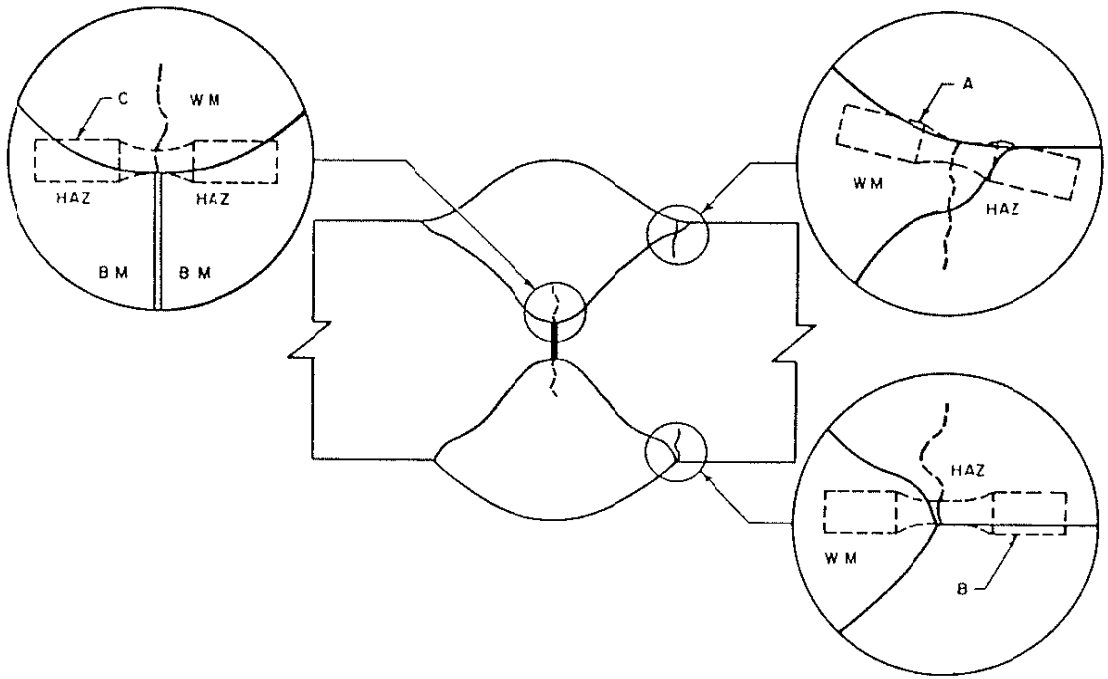


Fig. 1 Typical locations of fatigue crack initiation in a butt weld. Fatigue cracks can initiate: in diluted, untempered weld metal (A); in the heat-affected-zone close to the line of fusion (B); and in tempered weld metal (C). The dashed-in fatigue specimens are laboratory smooth specimens which, if subjected to the local strains, should initiate a fatigue crack at the same life as the region in question. From Higashida [2].

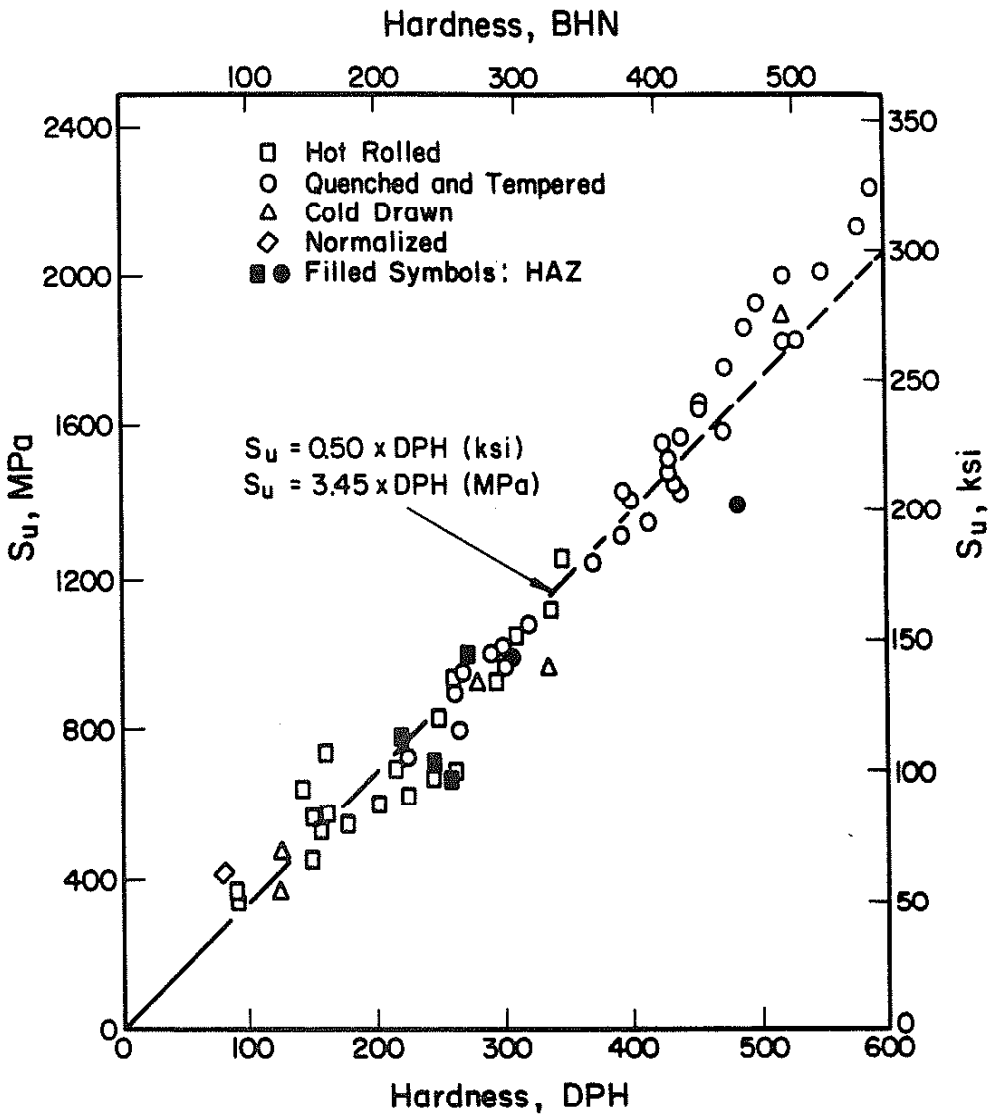


Fig. 2 Ultimate Tensile Strength as a Function of Hardness.

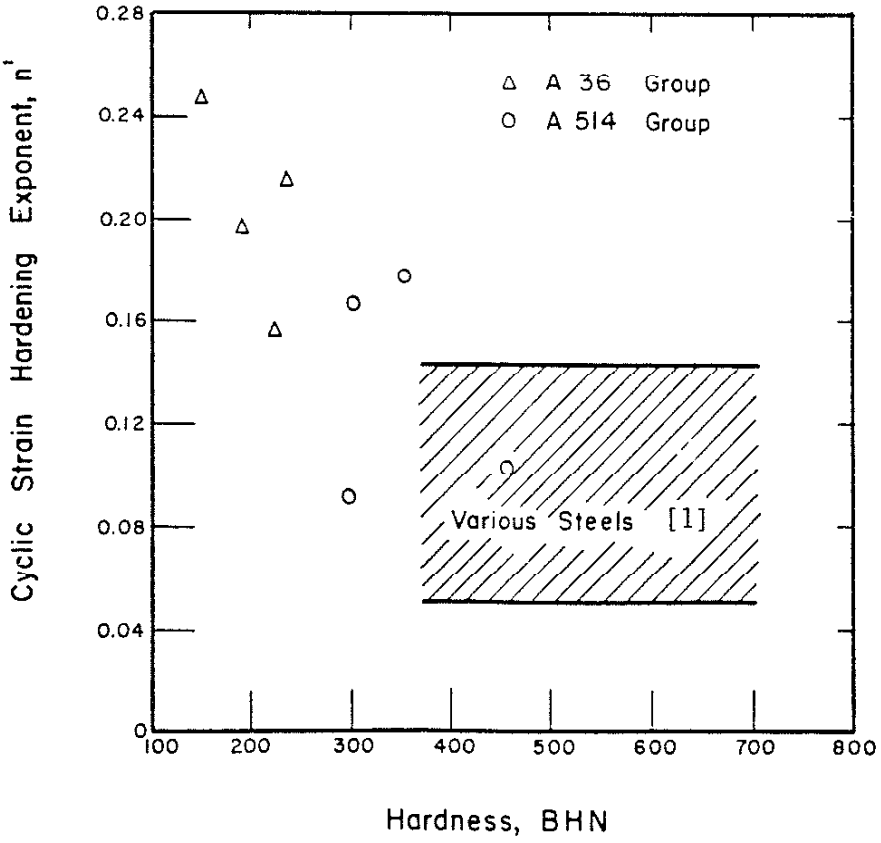


Fig. 3 Cylic Strain Hardening Exponent, n', as a Function of Hardness. From Higashida [2].

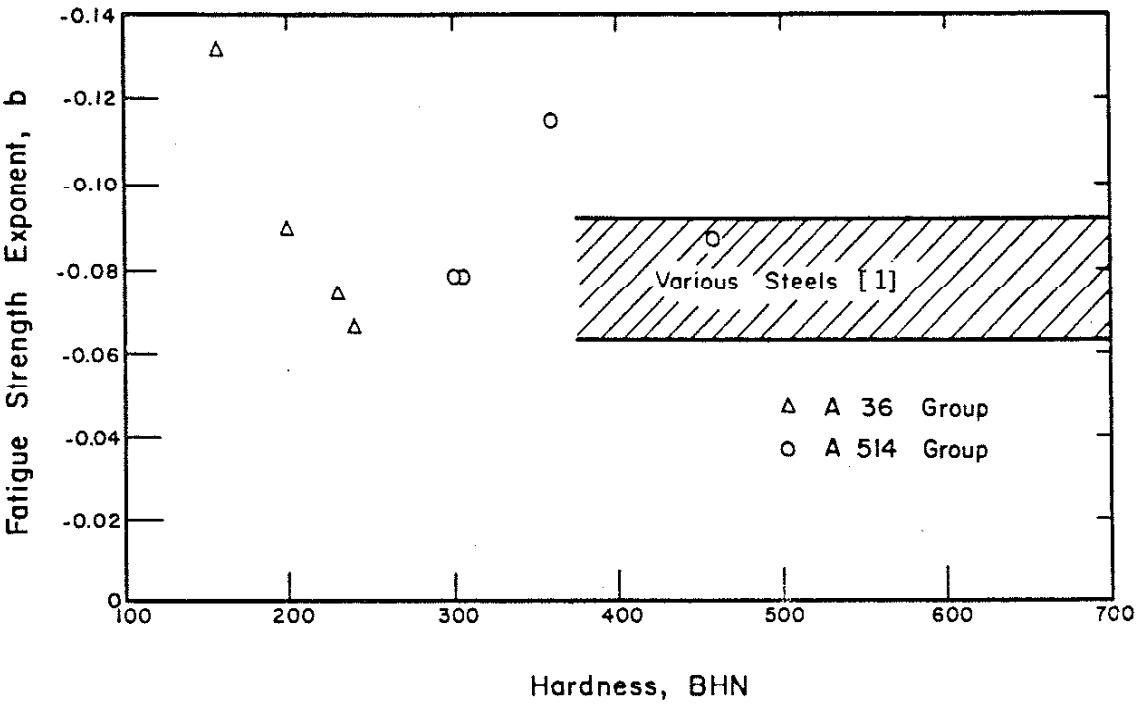


(a)

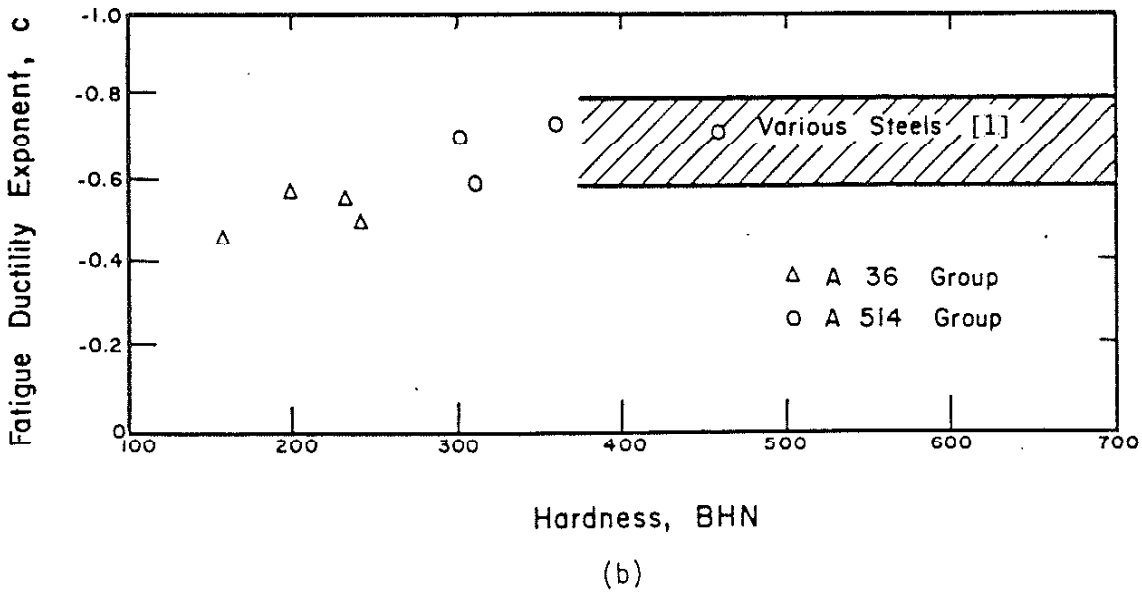


(b)

Fig. 4 Fatigue Life Exponents as Functions of Hardness:
(a) Fatigue Strength Exponent as a Function of Hardness
(b) Fatigue Ductility Exponent as a Function of Hardness
From Higashida [2]

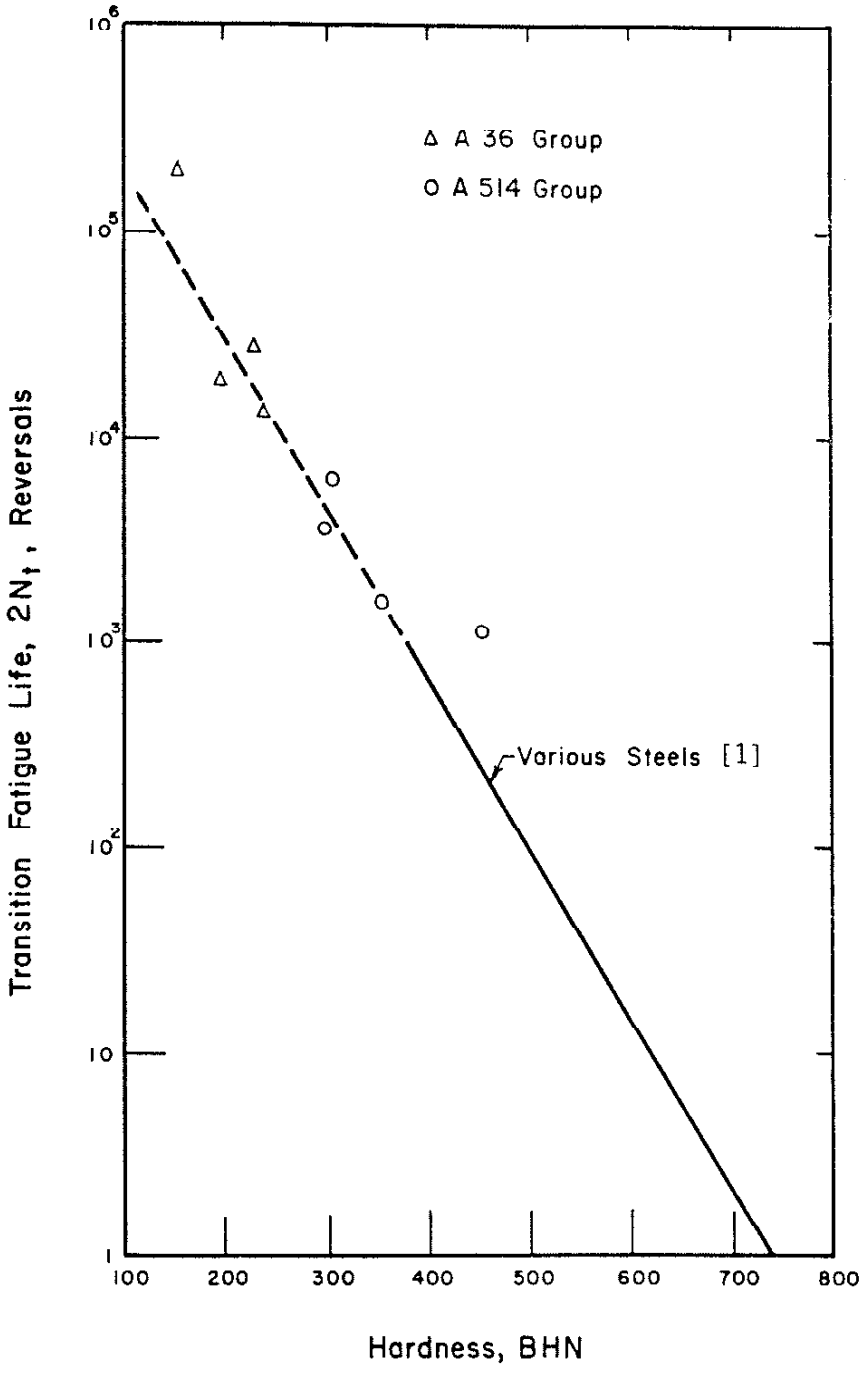


Fig. 5 Transition Fatigue Life as a Function of Hardness. From Higashida [2].

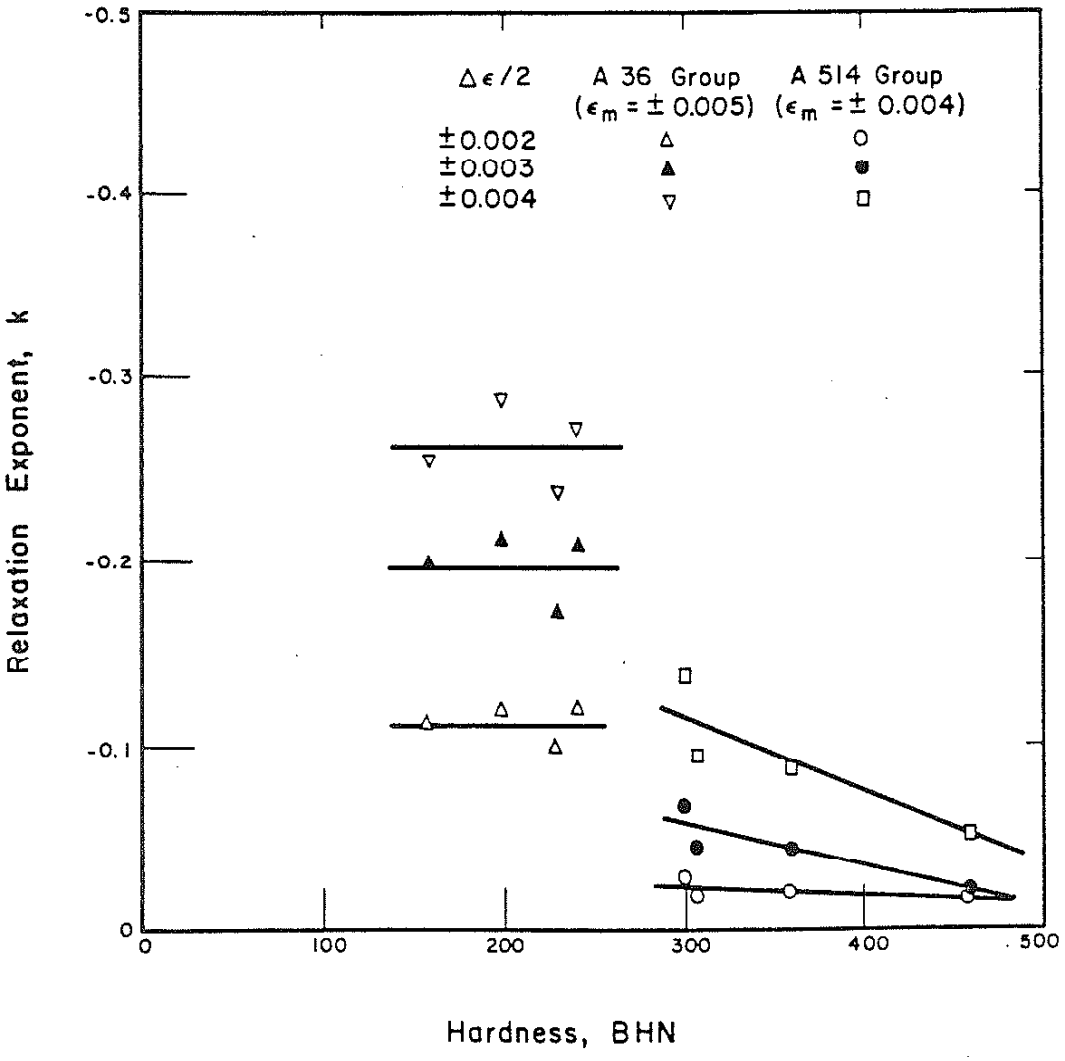


Fig. 6 Relaxation Exponent as a Function of Hardness. From Higashida [2].

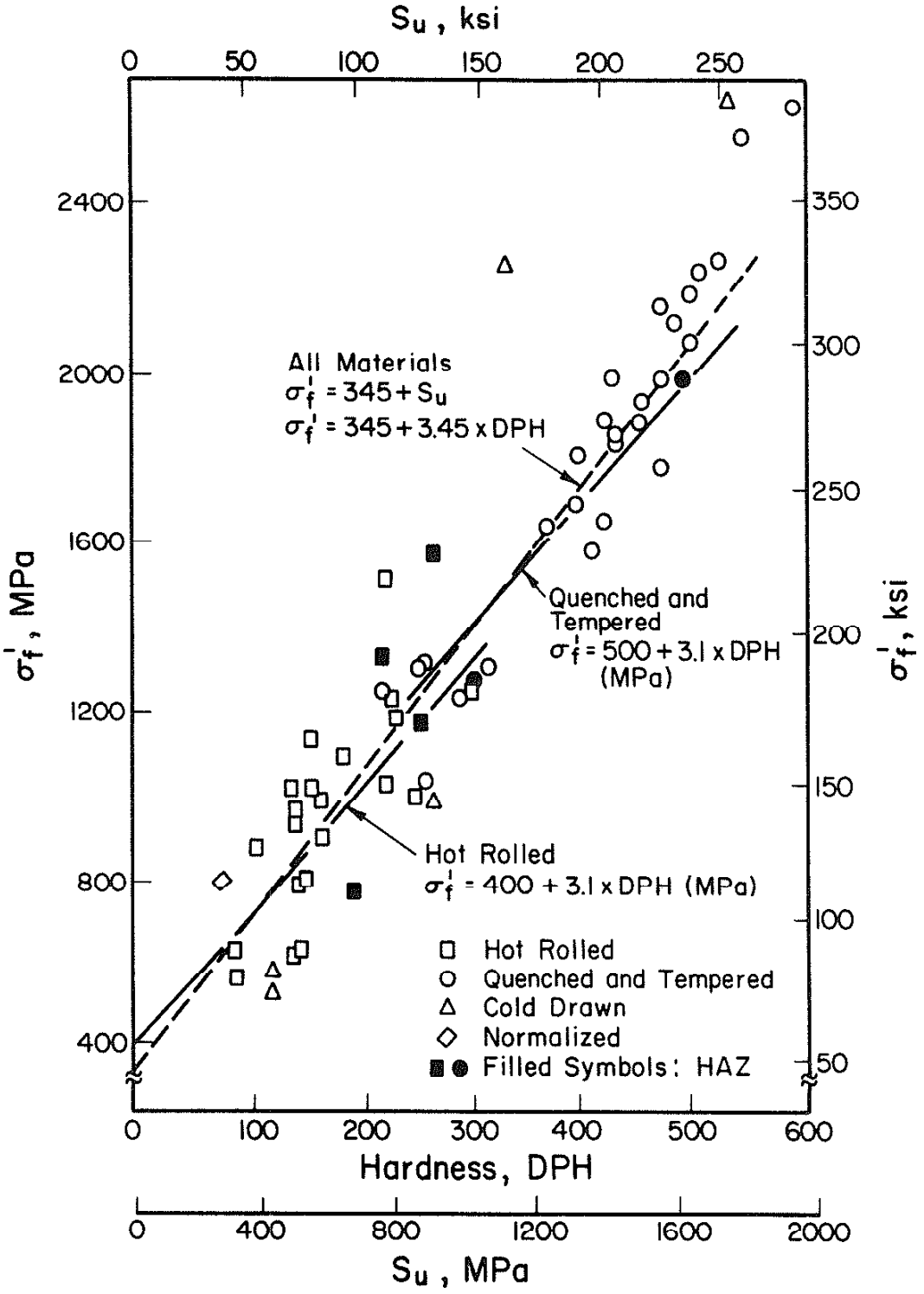


Fig. 7 Fatigue Strength Coefficient as a Function of Hardness.

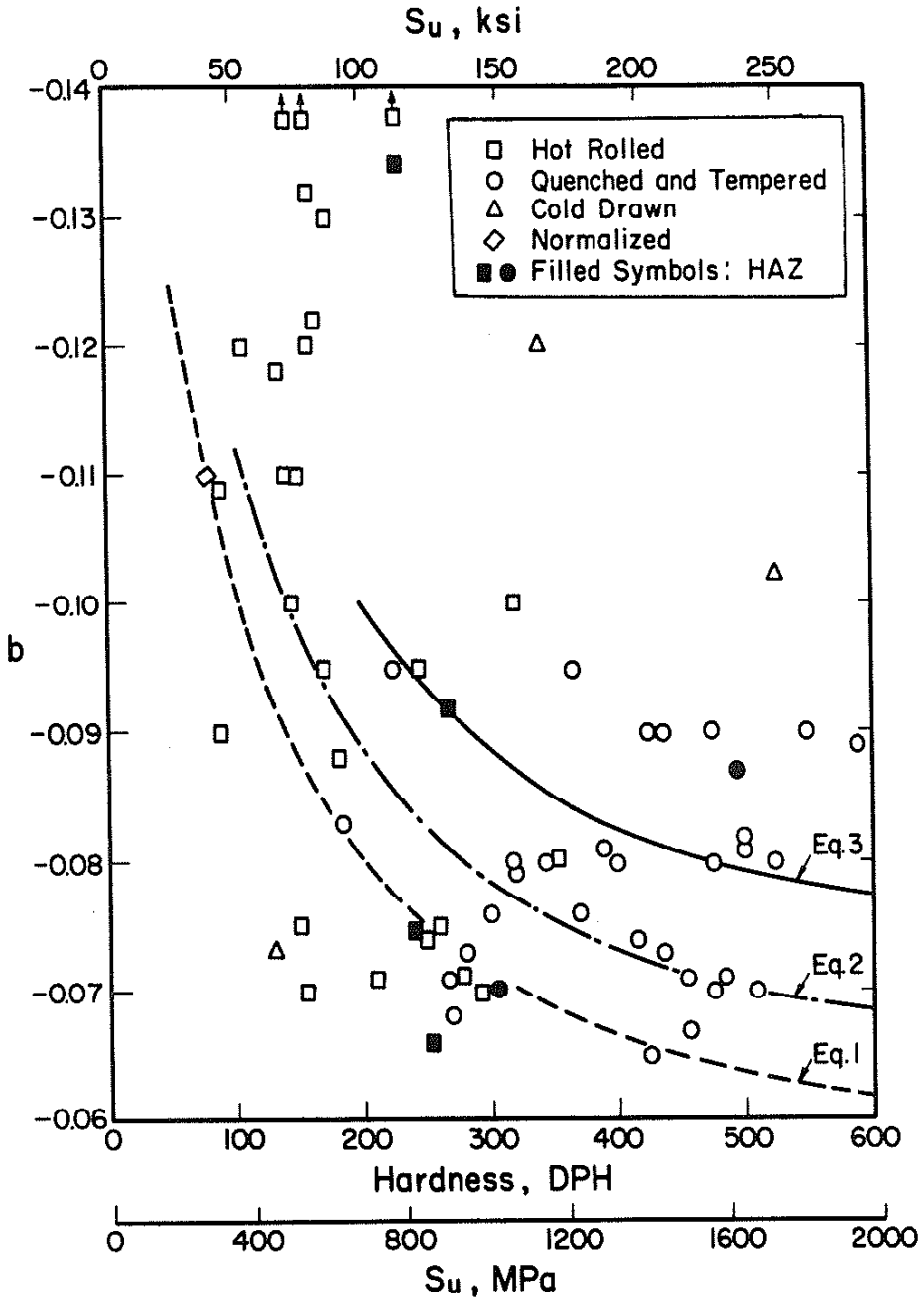


Fig. 8 Fatigue Strength Exponent as a Function of Hardness. Eqs. 1 - 3 are explained in Section 2.3 of the text.

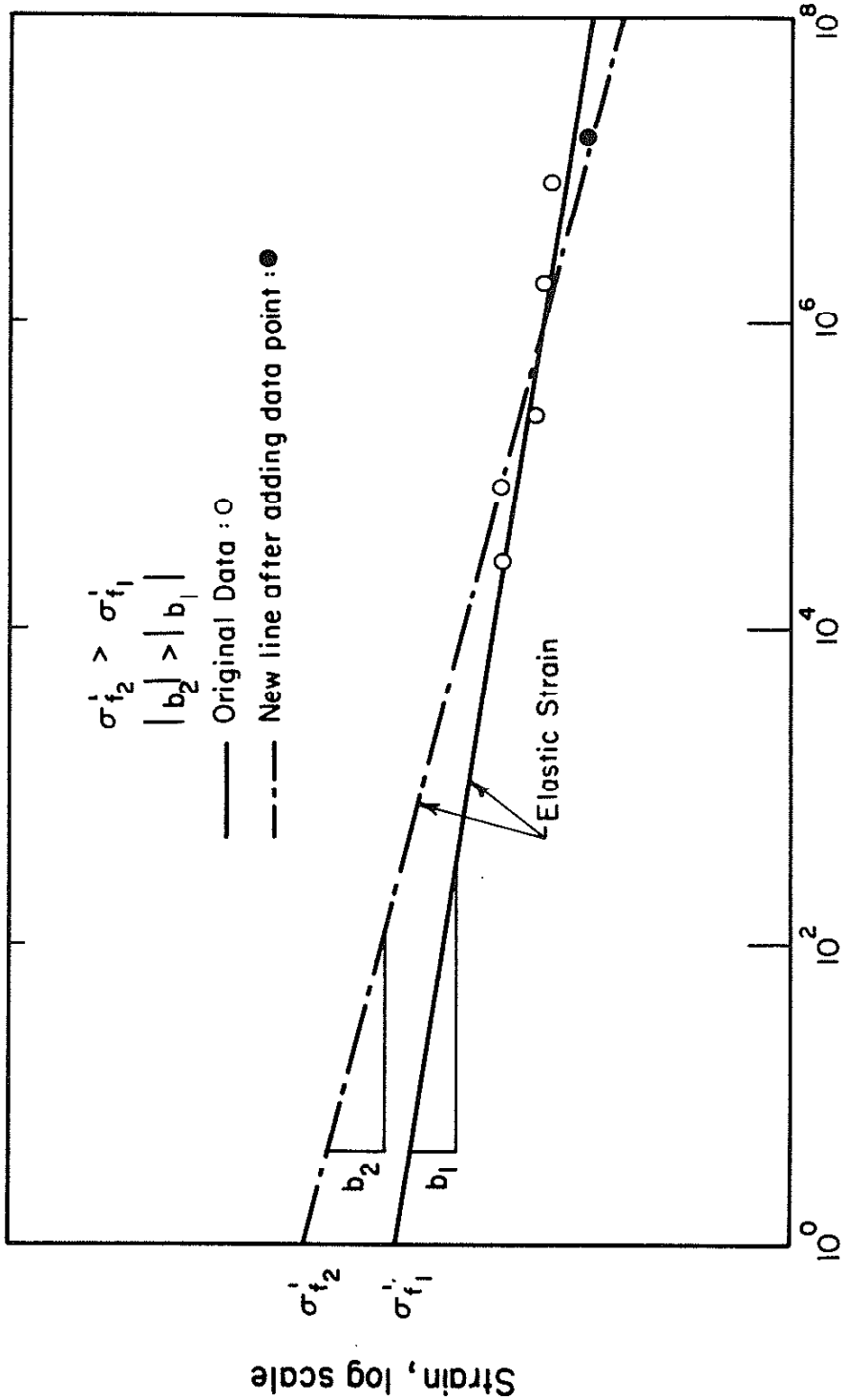


Fig. 9 Coupled Changes of the Fatigue Strength Coefficient and Exponent with the Addition of a New Data Point.

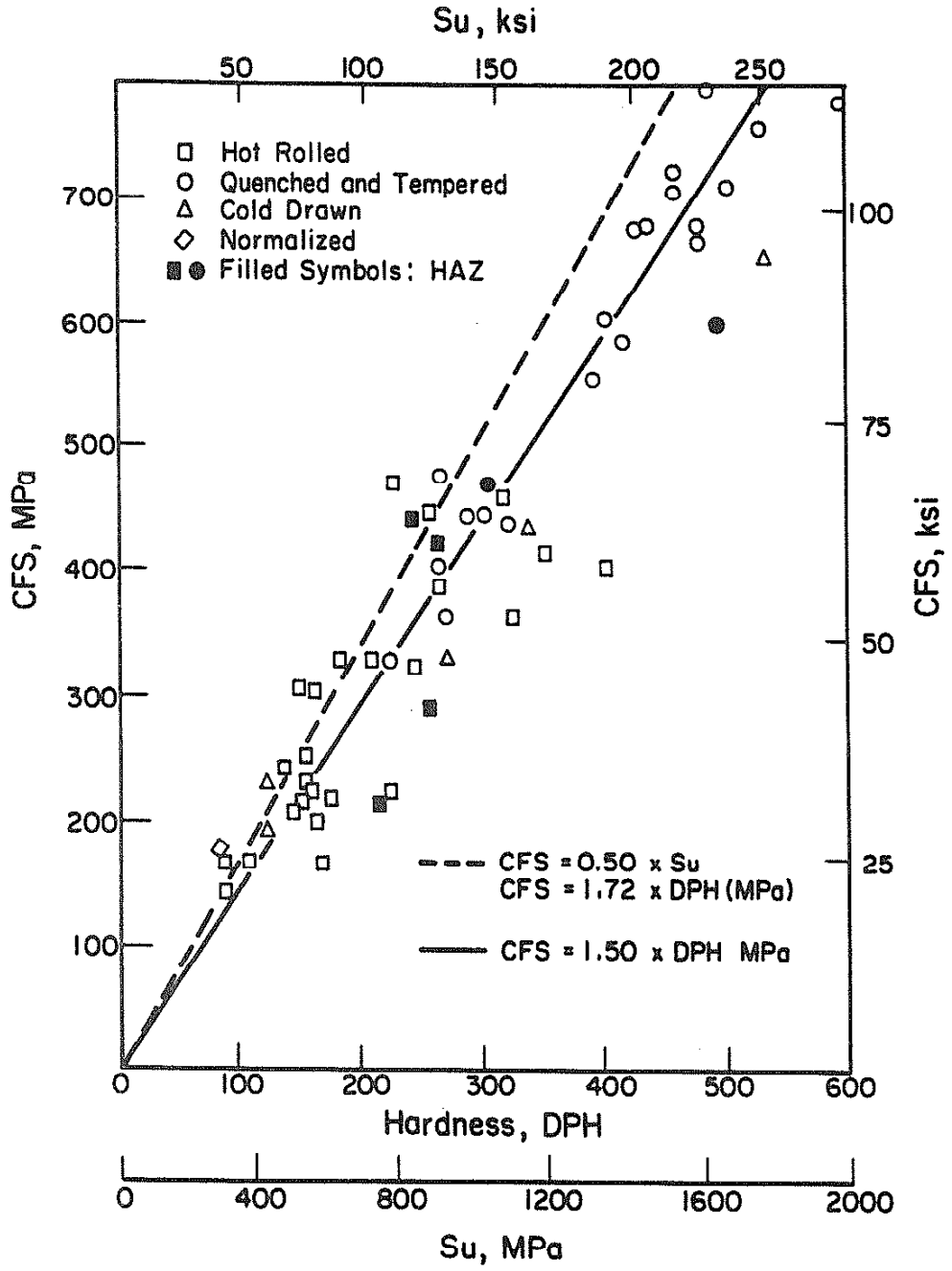


Fig. 10 Calculated Fatigue Strength at $10^6$ Reversals as a Function of Hardness.

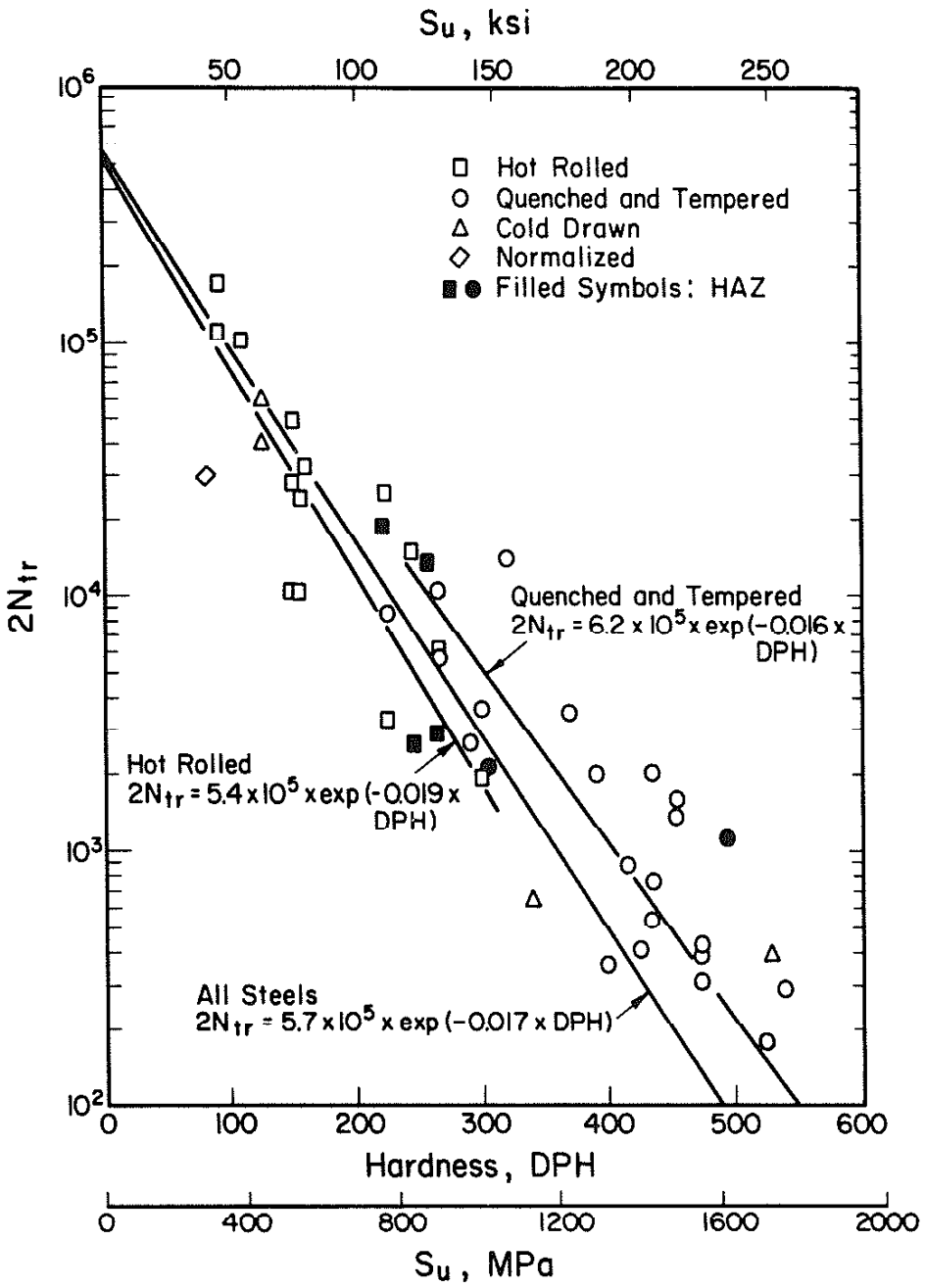


Fig. 11 Transition Fatigue Life as a Function of Hardness.

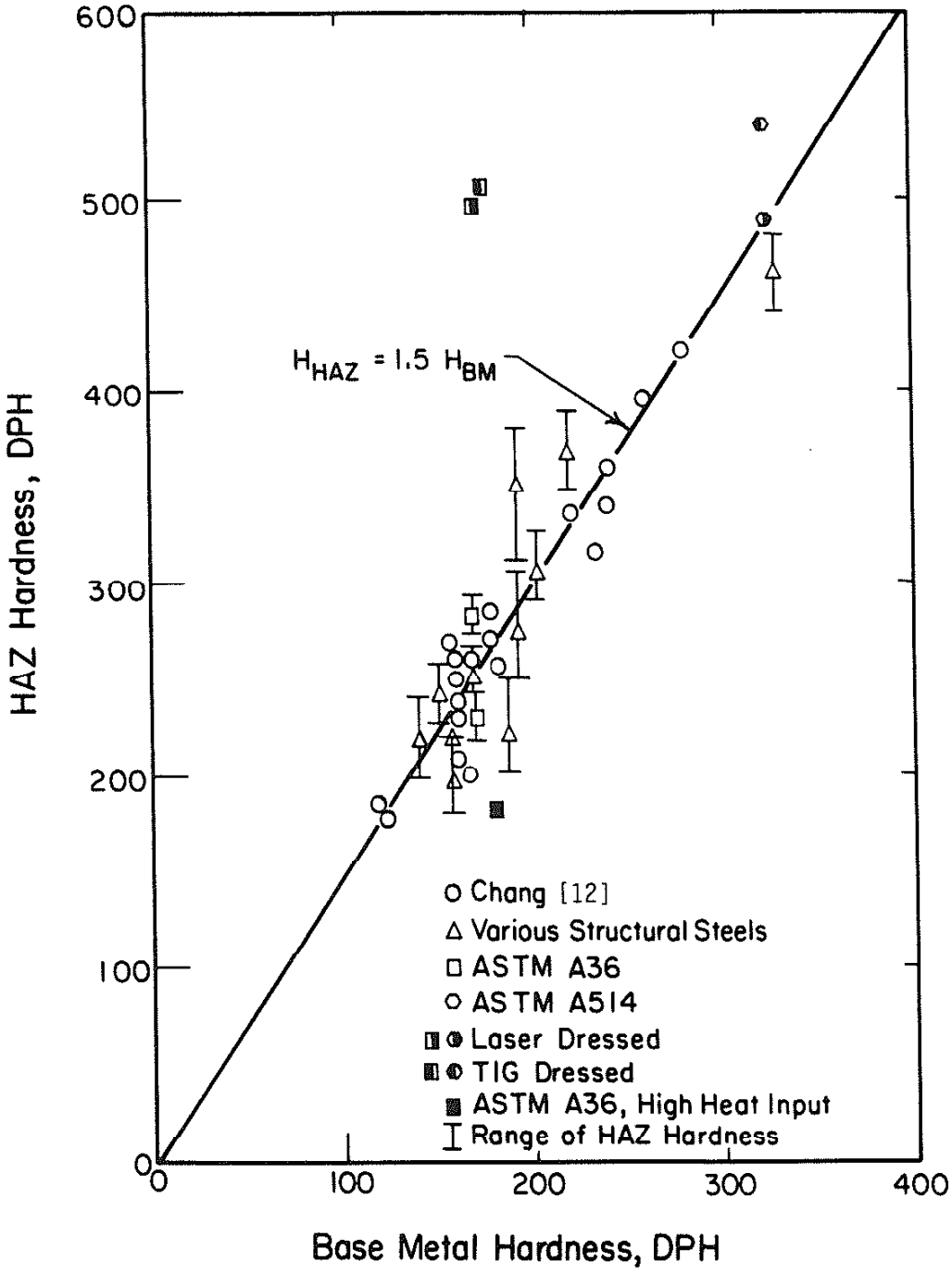


Fig. 12 Hardness of the Heat-Affected-Zone (HAZ) as a Function of Base Metal (BM) Hardness.

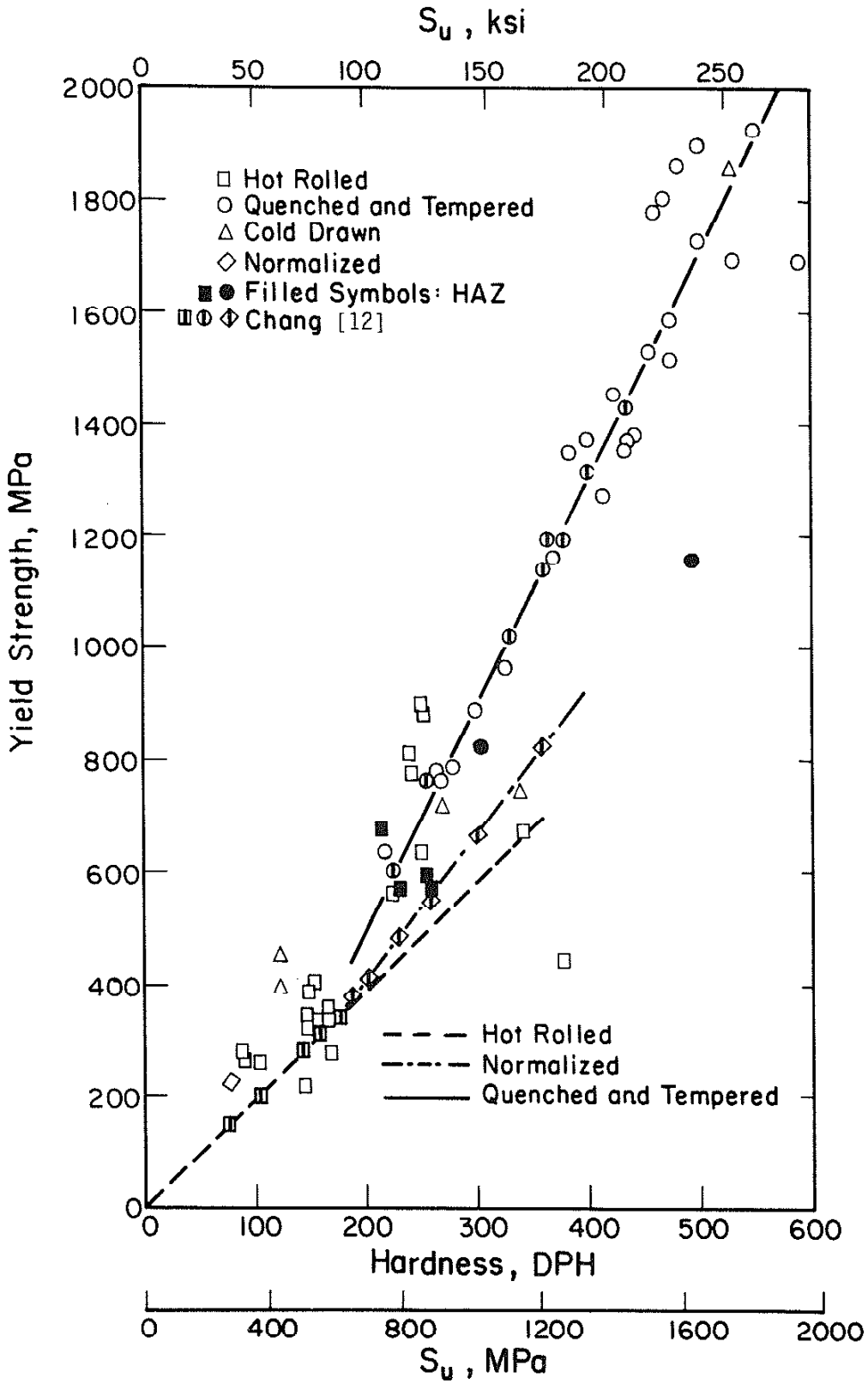


Fig. 13 Yield Strength as a Function of Hardness.

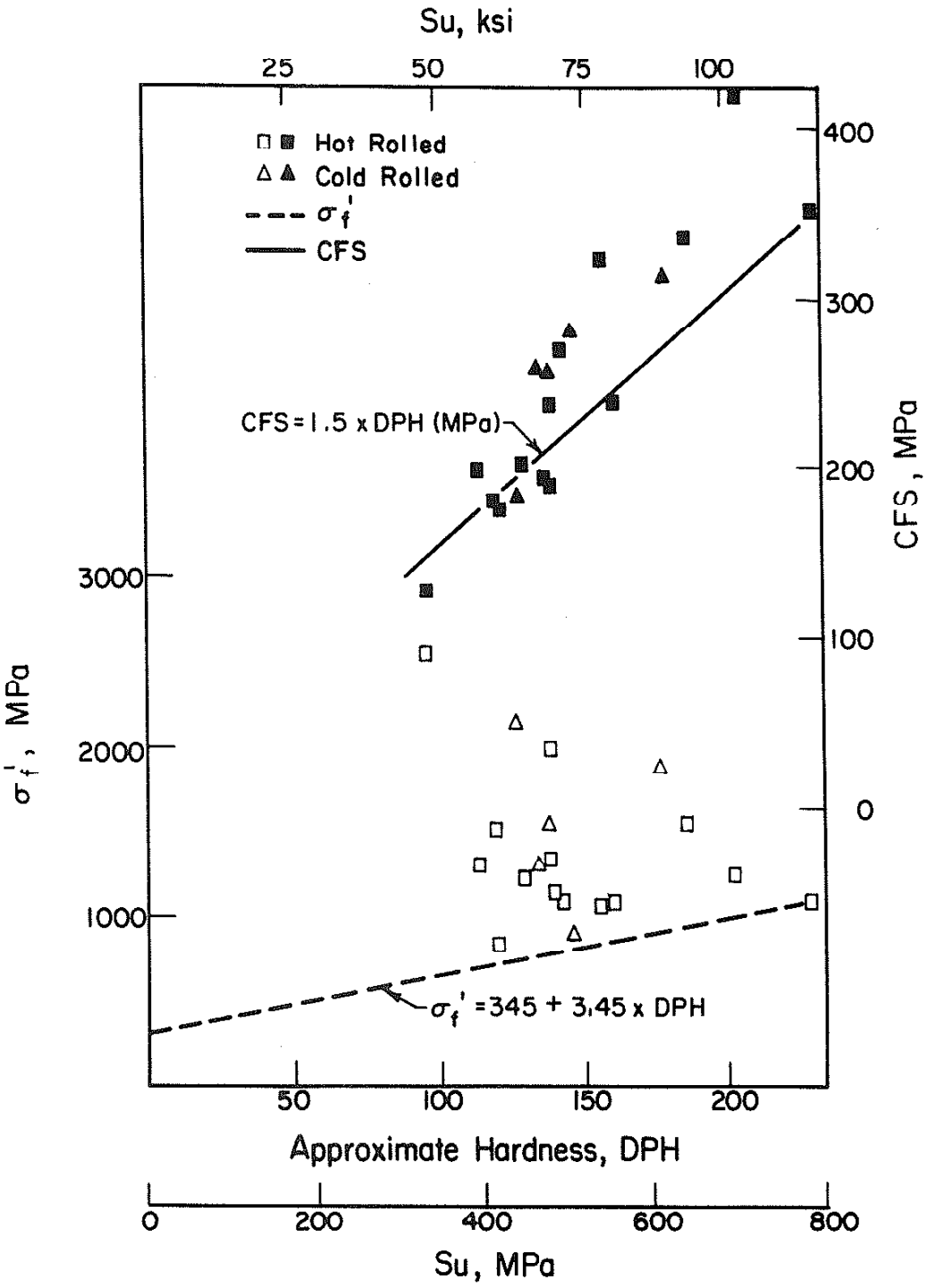


Fig. 14 Fatigue Strength Coefficient and Calculated Fatigue Strength (CFS) for Thin Sheet as Functions of Approximate Hardness. Data from Miller et al. [13].

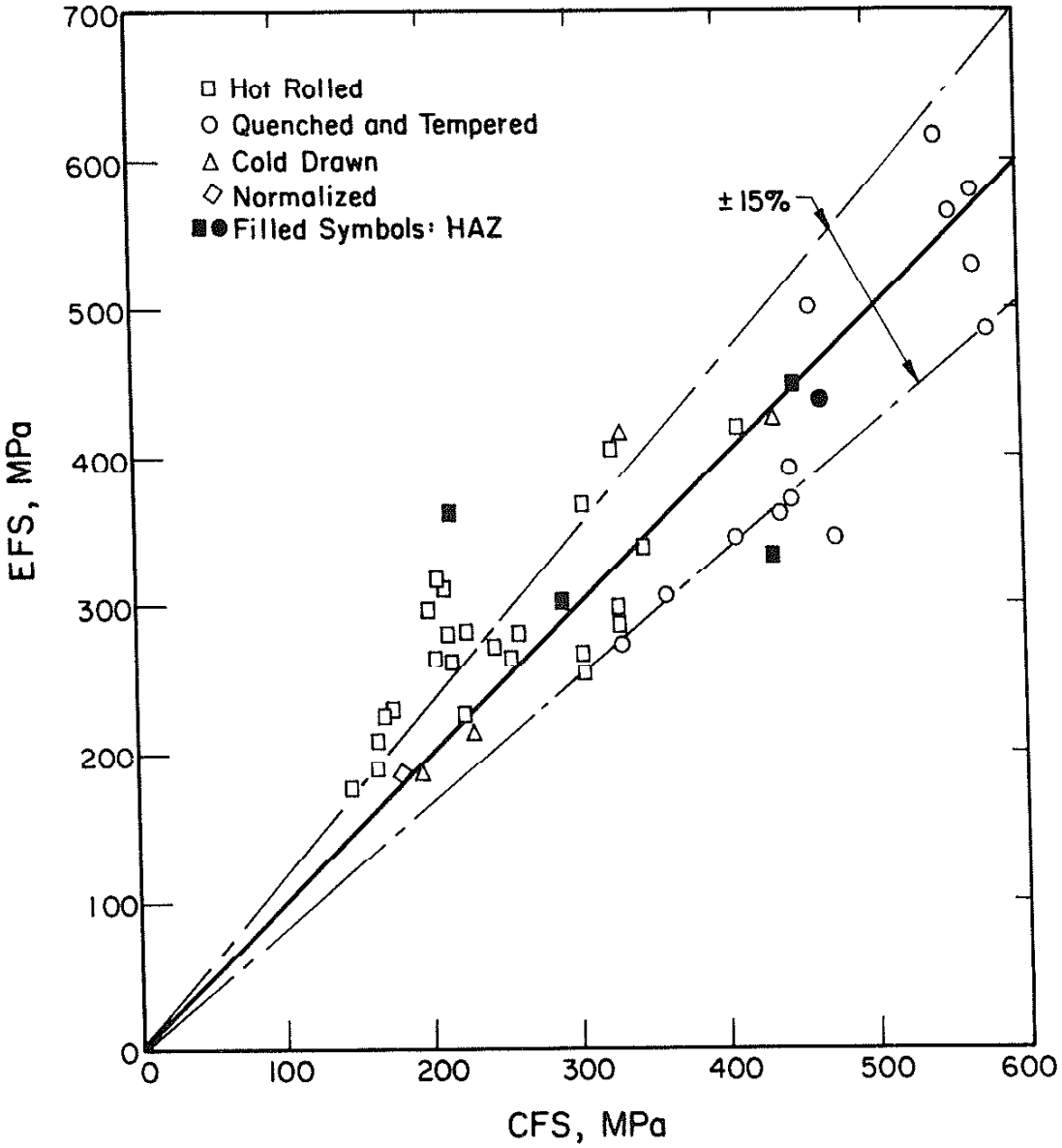


Fig. 15 Comparison of the Estimated Fatigue Strength (EFS) and the Calculated Fatigue Strength.